

OPTIMAL CHARACTERISATION OF WELD LINES AND VALVE LOCATIONS IN A THIN-WALLED CYLINDRICAL PRESSURE VESSEL USING FINITE ELEMENT ANALYSIS

¹Grannon, M., ¹Habibi, H.*

¹School of Computing, Engineering, and Digital Technologies, Teesside University,
Middlesbrough TS1 3BX, United Kingdom.

* Corresponding Author: H.Habibi@tees.ac.uk TEL: (+44)-1642342483

Received: 06 January 2024; Accepted: 27 December 2024; Published: 31 December 2024

doi: 10.35934/segj.v9i2.98

Highlights:

- Optimal valve placement for maximum stability
- Analysis of weld design for superior structural integrity
- Enhanced safety through component reconfiguration

Abstract: This paper addresses the critical problem of optimizing weld geometry and valve location in pressure vessel to minimize stress concentration and enhance structural integrity. The study focuses on a thin-walled pressure vessel with a cylindrical body and a spherical head, analysing how different weld and valve configurations impact the stress distribution. The design adheres to the ASME Boiler and Pressure Vessel Code IX, with steel as the base material and EX80XX for the welds. The objectives are to identify the safest weld arrangement and the optimal valve location to reduce structural risks. A combination of theoretical stress analysis and Finite Element Analysis (FEA) was used to evaluate the pressure vessel under a uniform internal pressure of 2 MPa. The study investigated seven valve positions and four weld lines arrangement. Results show that placing the valve at the centre of the spherical head minimizes the stress concentration, while the safest weld configuration is a single weld line at the interface between the cylindrical and the spherical sections. The study further explores the combined effects of multiple valves and weld lines, concluding that placing valves and welds in the cylindrical section increases structural risk compared to the spherical section. This research offers novel insights into the design of pressure vessel, offering optimal weld and valve configurations to enhance safety and performance.

Keywords: pressure vessel; optimal design; weld lines; valve location; finite element analysis

1. Introduction

A pressure vessel, essential in various industries such as oil and gas, manufacturing, and healthcare, serves as a container designed to store or handle fluids under either positive or negative pressure relative to the atmosphere. Enduring extreme temperatures and pressures throughout its operational lifespan is typical for these vessels. Diverse in design and material composition, pressure vessel is tailored to specific applications and operational requirements. Compliance with stringent regulations, such as those set forth by the American Society of Mechanical Engineers (ASME) or the British Standards Institution (BSI), governs crucial aspects including shell thickness, material selection, and manufacturing processes, ensuring their safety and longevity (Spence & Tooth, 1994).

However, the complexity of modern pressure vessel poses challenges in accurately predicting potential failures solely through stress calculations. To address this, Finite Element Analysis (FEA) has emerged as a prevalent method for simulating loading effects and identifying stress concentration points. FEA employs numerical techniques and simultaneous algebraic equations to conduct structural analysis, heat transfer assessments, and fluid flow simulations (Logan, 2017). Niranjana *et al.* (2018) carried out a study to identify how to design a pressure vessel using ASME codes and FEA. They demonstrated that FEA could be used to accurately represent stress values in a vessel under an internal pressure. Diamantoudis & Kermanidis (2005) compared the design by FEA analysis of a pressure vessel with theoretical equations for maximum permissible pressure and stress to determine the accuracy between these two methods. Romero-Tello *et al.* (2025) utilized genetic algorithms integrated with FEA to optimize pressure hull structures, focusing on weight reduction while ensuring compliance with Det Norske Veritas (DNV) standards. Also, Solangi *et al.* (2024) conducted stress analyses on vacuum pressure vessels using FEA, emphasizing material selection and geometric considerations to enhance structural integrity under operational conditions. Another research explored optimization techniques like the Taguchi method and genetic algorithms to enhance boiler performance through improved pressure vessel design (Singh *et al.*, 2023).

A common way to join parts together in a pressure vessel is welding which should form a strong mechanical joint and ensures minimal risk of failure. It is also less labour intensive than other methods such as riveting (Hodge, 1936). However, welding as a process involves massive amount of heat and energy to fuse two materials together which usually cause residual stress and strain in a component. FEA simulation could be also used to predict stress distribution and

failure risk caused by welding. The work by Fricke *et al.* is a representative study to illustrate how residual stress can cause damage or failure of components while presenting the FEA technique as an effective tool to predict residual stress and simulate welds in pressure vessel (Fricke *et al.*, 2001). In this present study, we compare different patterns employing weld lines in designing and manufacturing pressure vessel which would lead to minimal residual stress in them.

Also, Kshitij & Sankalp (2019) studied the impact of geometric parameters on the increase of stress generated under a point force on a welded joint using FEA technique. Their findings highlighted that the maximum stress occurs at the sharp intersection between the weld and the component.

Despite extensive research efforts, a significant number of failures resulting in injuries and fatalities occur annually. A study by Ladokun *et al.* (2010) revealed 23,338 pressure vessel-related accidents from 1992 to 2001. Given the wide-ranging applications of pressure vessel across various contexts, their failure modes can vary significantly. Common causes of failure include stresses (such as pressure, thermal, bending, and compressive), cracking, welding defects (including porosity, material flaws, and voids), elastic deformation, and brittle fracture (Moss, 1987).

The aim of this paper is to demonstrate how the selection of weld lines arrangement and valve locations affect the stresses created in a pressure vessel and characterise the optimal geometry using a combination of theoretical computation and FEA simulation. The technical information derived out of results and findings of this study could be used to improve the design and reduce the failure risk of pressure vessel under positive internal pressure.

2. Modelling a Pressure Vessel

2.1. Assumptions

To verify the viability and accuracy of FEA method for simulating a pressure vessel under internal pressure, a base model of pressure vessel (i.e. the model without nozzle and weld) was designed as the first step. By employing theoretical principles, it becomes feasible to ascertain the maximum principal stresses experienced by the pressure vessel. Subsequently, these findings must undergo validation via Finite Element Analysis (FEA) to ensure the accuracy of the simulated model. Once the FEA validation is completed successfully, the model can then be employed to investigate how the placement of welds and valves influences the stress levels within a thin-walled pressure vessel.

The assumptions inherent in the theoretical computation and modelling process of this study include:

- The absence of external pressure acting on the vessel.
- No application of thermal gradients to the vessel.
- All materials are assumed to be isotropic and homogeneous.
- Absence of a heat-affected zone resulting from welding.
- Uniform pressure distribution across the internal surface of the pressure vessel.

2.2. Methodology

2.2.1. Theoretical Background

As well known, three principal stresses in a cylinder under internal pressure occur which are longitudinal stress, hoop stress and radial stress. To carry out the stress analysis in a thin-walled vessel, a base model (without weld line and valve bore) was first created using NX 12 software as shown in **Figure 1**.

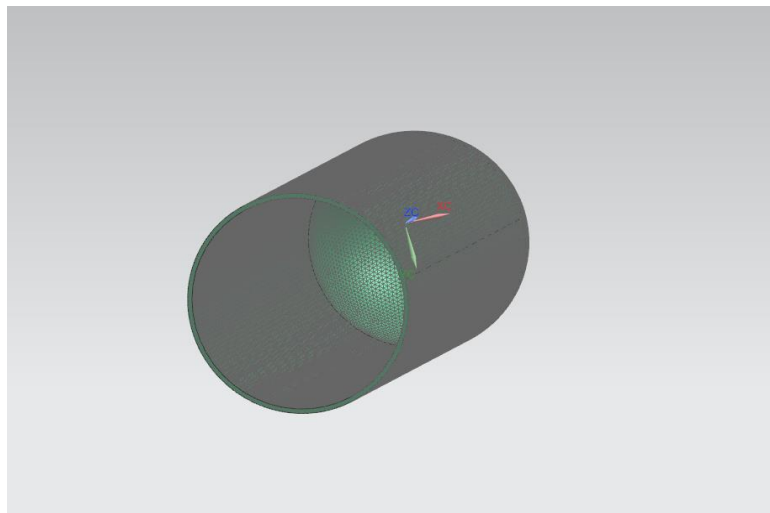


Figure 1. Basic design of pressure vessel created on NX 12 software

The vessel is subjected to a 2 MPa internal pressure. Other properties of the vessel are listed in **Table 1**.

Table 1. Properties of the pressure vessel

External diameter of cylindrical section (mm)	500
Length of cylindrical section (mm)	1000
External diameter of spherical section (mm)	500
Material	ASIS 1040 Steel

Youngs modulus (GPa)	200
Poisson's ratio	0.29

To guarantee compliance with ASME boiler and pressure vessel design standards, it is imperative to calculate the minimum allowable thicknesses for both the spherical head and cylindrical sections of the pressure vessel through

$$t_{cyl} = \frac{PR}{SE - 0.6P} \quad (1)$$

$$t_{sph} = \frac{PR}{2SE - 0.6P} \quad (2)$$

where t_{cyl} is cylindrical shell thickness, t_{sph} , spherical head thickness, P , working pressure, R , external radius (inch), S , stress value of material (Psi) and E is joint efficiency (Megyesy, 2001). As there is no weld in the model, the joint efficiency is assumed to be 1.

The minimum wall thickness for the pressure vessel to meet ASME standards were then obtained using equations (1) and (2), and the values are presented in **Table 2**. Nevertheless, the effect of factor of safety needs to be also contributed in the results to comply with the standard regulations for pressure vessel. Having chosen the factor of safety as 2 in this study, the vessel thickness is then worked out as 5 mm, giving the vessel an internal diameter of 490 mm. The maximum principal stresses in the vessel are also determined through

$$\sigma_L = \frac{PD}{4t} \quad (3)$$

$$\sigma_H = \frac{PD}{2t} \quad (4)$$

where σ_L is the longitudinal stress, σ_H , the hoop stress, P , internal pressure, D , diameter, and t is the wall thickness (Megyesy, 2001). The principal stresses obtained using equations (3) and (4), and the values are presented in Error! Reference source not found.. When determining the hoop and longitudinal stress within the spherical head of the pressure vessel, it is reasonable to assume that these stresses are equal. This equality arises from the constant curvature of the sphere, as outlined by Moss (1987).

Table 2. Minimum wall thickness of the pressure vessel sections

Pressure vessel section	Minimum wall thickness (mm)
Cylindrical	2.512
Spherical	1.249

Table 3. Maximum principal stress calculated for the cylindrical and spherical sections of the pressure vessel

Cylindrical hoop stress	50 MPa
Cylindrical longitudinal stress	100 MPa
Spherical hoop stress	50 MPa

2.2.2. FEA Simulation and Verification of Results

The pressure vessel model was constructed using Siemens NX 12, maintaining the same dimensions as those utilized in the theoretical approach. To expedite simulation runtime, only half of the pressure vessel was modelled along the Z-axis. This approach does not compromise modelling accuracy due to the vessel's symmetry about the XY plane, while significantly reducing computational time.

A 3D tetrahedral mesh with a size of 20 mm and 10 nodes was chosen. The mesh was assigned a base material of steel. To constrain the pressure vessel, a "user-defined constraint" was applied, focusing on the open edge of the vessel as illustrated in **Figure 2**. Since the pressure vessel remained open at one end, the model was designed to allow expansion in the "X", "Y" (cross-sectional), and "T" (theta) directions while being fixed in the "Z" (longitudinal) direction. A uniform pressure of 2 MPa was applied to the internal surface of the vessel.

The simulation is subject to the following limitations: thermal gradients were not applied to the vessel in this analysis; the heat-affected zone from welding was not included in the simulation; all materials were modelled as isotropic and homogeneous, without considering material anisotropy or heterogeneity; and the internal pressure was assumed to be uniformly distributed across the entire surface of the pressure vessel, without variation.

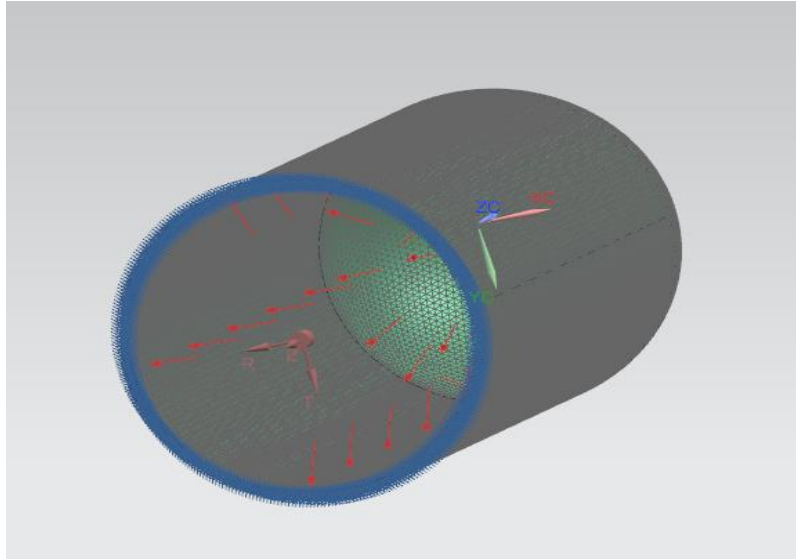


Figure 2. The base pressure vessel with the constraint applied to the edge of the vessel

After applying constraints to the pressure vessel and introducing pressure, the simulation could proceed. Subsequently, the maximum principal stresses were documented for both the spherical and cylindrical sections. Various mesh sizes and types were employed to assess their impact and determine how they might influence the maximum principal stresses, providing a comparative context against the theoretical results outlined in **Table 3**. Maximum principal stress calculated for the cylindrical and spherical sections of the pressure vessel

According to the theory-based results presented in **Table 3**, the maximum stress occurs in the cylindrical section of the pressure vessel is 100 MPa. This value was verified using FEA modelling with different mesh sizes and types as detailed in **Table 4**

Table 4. Results derived from the simulations of the base pressure vessel

Mesh Type	Mesh Size (mm)	Number of Nodes	Maximum Stress (MPa)	Run time (s)	Accuracy Compared with Theoretical Value
3D TET	20	10	97.54	12	97.54%
3D TET	10	10	98.02	35	98.02%
3D TET	5	10	98.75	192	98.75%
3D TET	3	10	99.28	395	99.28%
3D SWEPT	20	20	96.21	12	96.21%

3D SWEPT	10	20	97.31	31	97.31%
3D SWEPT	5	20	97.48	92	97.48%
3D SWEPT	3	20	97.62	426	97.62%

As inferred from **Table 4**, using the 3D tetrahedral mesh with 10 nodes and the mesh size of 3mm results in the best agreement between FEA modelling and theoretical computation. It could also be seen that the results converged at a 10 mm mesh size.

Upon comparing the 3 mm mesh with the 5 mm mesh, it was noted that although there was only a marginal difference in accuracy (0.53%), the computational time nearly doubled. Similarly, contrasting the tetrahedral mesh with the swept mesh revealed that the tetrahedral mesh yielded results closer to the theoretical calculations. In light of these initial observations, it was determined to proceed with FEA simulation employing a 3D tetrahedral mesh comprising 10 nodal points and a 5 mm mesh size for all subsequent testing. This decision stemmed from the mesh's high level of accuracy in comparison to theoretical values, coupled with its efficient computational performance. The computational efficiency will become more important in the new tests as the vessel geometry will be made more complex when including welds and valves. Furthermore, in such complex geometries, a tetrahedral mesh over a swept mesh would undergo less irregularities which leads to less computational cost and runtime.

3. Optimisation of Valve Locations

Valves serve the function of facilitating the filling or emptying of a pressure vessel, enabling the passage of a medium into or out of the vessel. However, the inclusion of a valve introduces changes to the vessel's geometry, thereby creating stress raisers. These stress raisers disrupt the uniform distribution of stress, resulting in increased stress values at these points.

3.1. Approach

To pinpoint the valve location that minimally affects the stress within the pressure vessel, seven distinct models were generated using NX software, as illustrated and outlined in **Figure 3** and **Table 5**. Consistent dimensions were maintained for the base pressure vessel throughout this phase of the study.

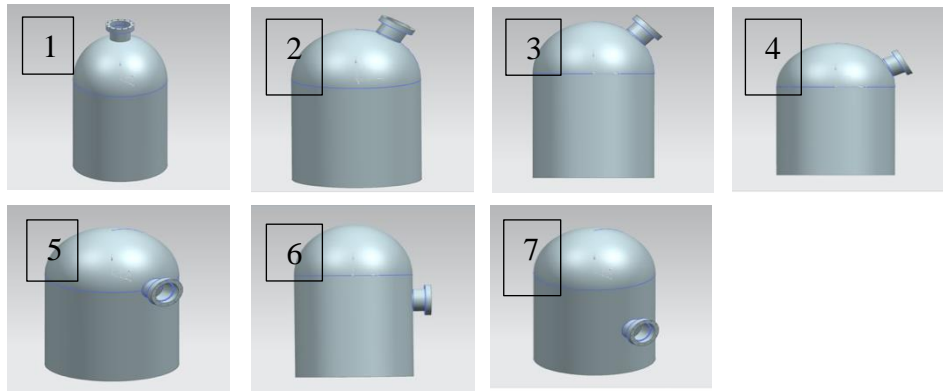


Figure 3. Seven different models created on NX, each model has a different valve location

Table 5. Measurements of the different valve locations

Valve model	Position
1	Centre of sphere
2	30 degrees from centre of sphere
3	45 degrees from centre of sphere
4	60 degrees from centre of sphere
5	90 degrees from centre of sphere
6	125mm from sphere/cylinder joint
7	250mm from sphere/cylinder joint

The valve bore's internal and external diameters were maintained at 100 mm and 110 mm, respectively, in adherence to ASME standards and to ensure consistency with the wall thickness of the pressure vessel. The mesh type utilized was 5mm, as indicated in the results of the base vessel, and the same material, constraint, and internal pressure were applied to the vessel walls.

3.2. Results and Discussion of Valve Location Optimisation

The data obtained regarding the maximum principal stress at the valve locations illustrates variations compared to the maximum stress at the same locations without the valve, as observed in the previous experiment. It was observed that stress levels increased at every location, indicating the presence of localized stress raisers at the intersection between the valve and the vessel body.

At the junction between the valve and the vessel wall, the stress reached its peak value. As stress measurements were taken farther away from the valve, a gradual reduction in stress was observed, indicating dissipation throughout the vessel, as depicted in **Figure 4**. These findings

align closely with the research conducted by Niranjana *et al.* (2018) and Bahadur *et al.* (2018). It was determined that the optimal location for the valve was within the spherical section. Additionally, when the valve was positioned within the spherical head of the vessel, the stress generated remained below the maximum principal stress of the cylinder section, which was 100 MPa without any perforations. Conversely, placing the valve within the cylindrical section of the vessel resulted in a significant increase in stress beyond the original stress value, as illustrated in **Table 6**.

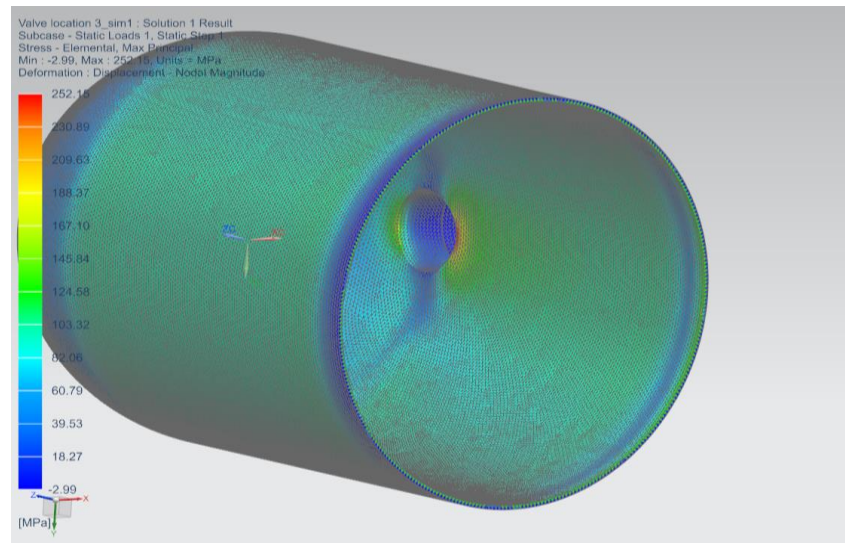


Figure 4. FEA results of a valve included in the pressure vessel

Table 6. Results recorded from the experiments detailing maximum stress at the valve and without a valve

Valve Location	Maximum Stress (MPa)	Original Stress at the Same Location Without Valve (MPa)	Increase in Stress (%)
1 (Sphere)	78.00	50	56.00
2 (Sphere)	80.20	50	60.40
3(Cylinder/sphere joint)	252.15	100	152.15
4 (Cylinder)	315.03	100	215.03
5 (Sphere)	87.25	50	75.05
6 (Sphere)	89.30	50	78.60
7 (Cylinder)	319.18	100	219.18

4. Multiple Valves in a Pressure Vessel

Given the data indicating that the inclusion of a valve in a pressure vessel leads to elevated principal stresses, it became pertinent to investigate whether the addition of multiple valves would exacerbate this stress.

4.1. Method

To assess the potential impact of introducing a second valve, a model was developed using NX 12, as shown in **Figure 5**. This model incorporated two valves within the spherical section and two valves within the cylindrical section of the vessel. Each valve location was systematically adjusted to determine if any alterations in stress levels occurred.



Figure 5. The NX model created to include second valve

4.1.1. Method for Cylindrical Multiple Valves

Within the cylindrical section of the vessel, an initial distance of 250 mm between valve centres was established, and the maximum principal stress values from the simulation were documented. Subsequently, the valves were incrementally moved closer by 10 mm, and a new simulation was conducted after each adjustment. This iterative process continued until a distance of 160 mm between valve centres was reached. Further measurements were not taken beyond this point due to interference between the valves occurring at 150 mm.

4.1.2. Method for Spherical Multiple Valves

In the spherical section of the vessel, two valves were positioned at 15° intervals from each other, commencing at 0° and 30° and concluding at 75°. At each interval, the maximum stress was recorded at the valve using the same method as described above. However, stress

measurements could not be obtained at 0° and 15° intervals between valves due to interference occurring at such close angles.

4.2. Results and Discussion for Multiple Valves

4.2.1. Cylindrical Section

Within the cylindrical section of the pressure vessel, it was observed that if the valve centres were positioned a minimum distance of 250 mm apart, there would be no additional increase in principal stress. The maximum stress recorded at a distance of 250mm was 315.37 MPa, which closely resembled the value recorded for a single valve in the cylindrical section of the vessel. Moreover, as displayed in **Figure 6**, a correlation was identified between the distance separating the valves and the effect on stress; as the distance increased, the principal stress at the valves decreased.

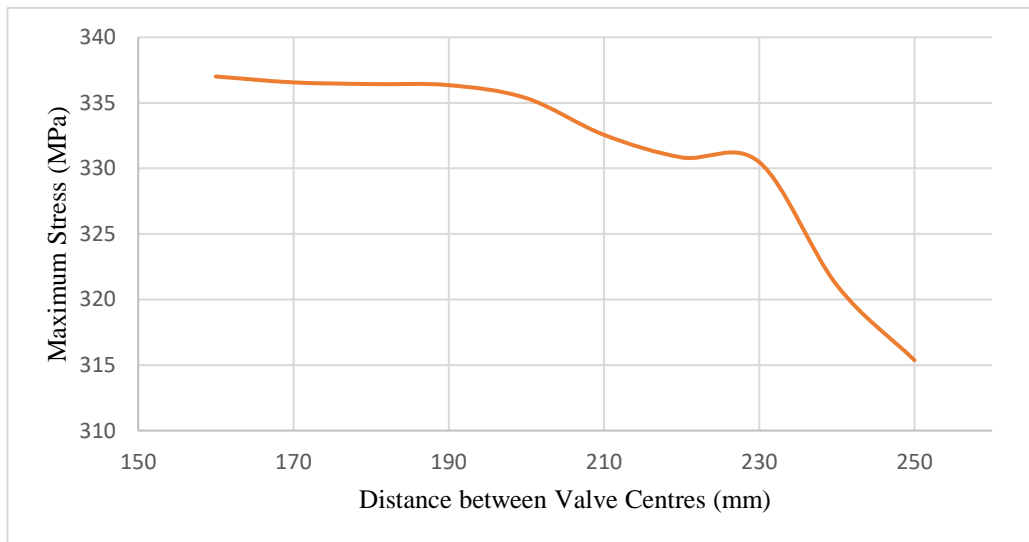


Figure 6. The correlation between the distance of the valves and the maximum principal stress

In the absence of additional valves, stress typically dissipates throughout the vessel, resulting in a normalization of stress levels. However, when a second valve is introduced near the first valve, as depicted in **Figure 6** and **Figure 7**, it becomes evident that the stress contours generated by both valves converge and fail to diminish, leading to interference. Consequently, this interference exacerbates stress within the vessel.



Figure 6. FEA result with valves in the cylindrical section 170 mm apart

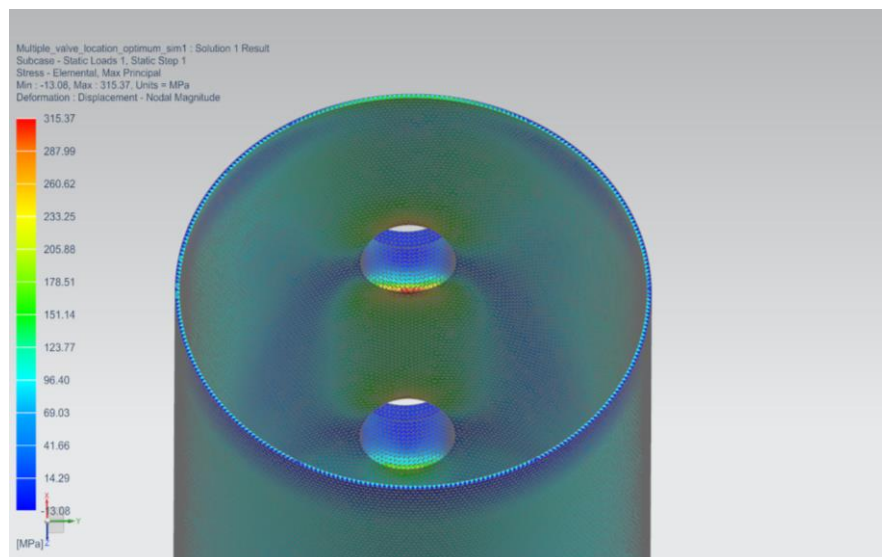


Figure 7. FEA results of two valves included in the cylindrical section 250 mm apart

4.2.2. Spherical Section

From the data collected from the spherical section, it could be seen again that having a second valve on the pressure vessel increased the principal stress recorded. It was found in the spherical section that there was no minimum distance between the valves to have no effect as in the cylindrical section.

The optimal placement for a second valve within the spherical section was found to be between 45° and 60° , with the maximum recorded stress value being 103.63 MPa. Notably, when the valves were positioned at their closest proximity, the greatest increase in stress was observed, as illustrated in **Table 7**. Results of FEA identifying maximum stress value recorded at the

valve at different spacings. However, an unexpected finding emerged when comparing the stress values between the 75° and 60° valve distances: despite the former being situated further away from the centre valve than the latter, the stress value was greater. This discrepancy was attributed to the valve location nearing the cylindrical section of the pressure vessel, resulting in an additional stress escalation.

A comparative analysis between the stress increases in the cylindrical and spherical sections revealed a higher percentage increase in the spherical section. Nevertheless, the actual stress generated remained significantly lower. Consequently, the optimal location for multiple valves in a pressure vessel was determined to be within the spherical section.

Table 7. Results of FEA identifying maximum stress value recorded at the valve at different spacings

Angle between Valve Centres	Maximum Principal Stress Recorded at Valves (MPa)
30°	157.76
45°	103.63
60°	103.63
75°	115.02

5. Weld Locations and Geometry

In pressure vessel manufacturing, welding stands as the predominant method for joining components, recognized for its safety (Hodge, 1936). Given its widespread use, understanding how welds influence stress distribution, particularly maximum principal stress, is crucial. Every manufacturing process imposes certain constraints on the design aspects of a pressure vessel, including weld line geometry and arrangement. To explore this phenomenon, four weld models were generated in Siemens NX, each representing common manufacturing techniques such as spinning, rolling, extrusion, and pressing (Pullarcot, 2002).

5.1. Method

Utilizing Siemens NX, four weld models were created of a pressure vessel with identical dimensions to those used in the previous experiments, as depicted in **Figure 8**. In order to simplify the pressure vessel and minimize simulation errors, a basic Butt weld was implemented. A new material was chosen for the weld component to align with the mechanical properties of EX80xx. These properties included a tensile strength of 551MPa, a yield strength

of 462MPa, and a percent elongation of 19 (Budynas *et al.*, 2011). This selection ensured that the simulation more accurately mirrored real-world manufacturing conditions.

To simulate the weld joints in NX 12, the "Surface to Surface Gluing" tool was utilized. This tool enables the user to select individual component faces and merge them together as welds. An "Override parameter" was activated, with "welded glue parameters" specified. The pressure vessel was subjected to the same internal pressure and constraint as in previous experiments to maintain consistency across simulations. This process was replicated for all four weld models, and the results for maximum principal stress were recorded.

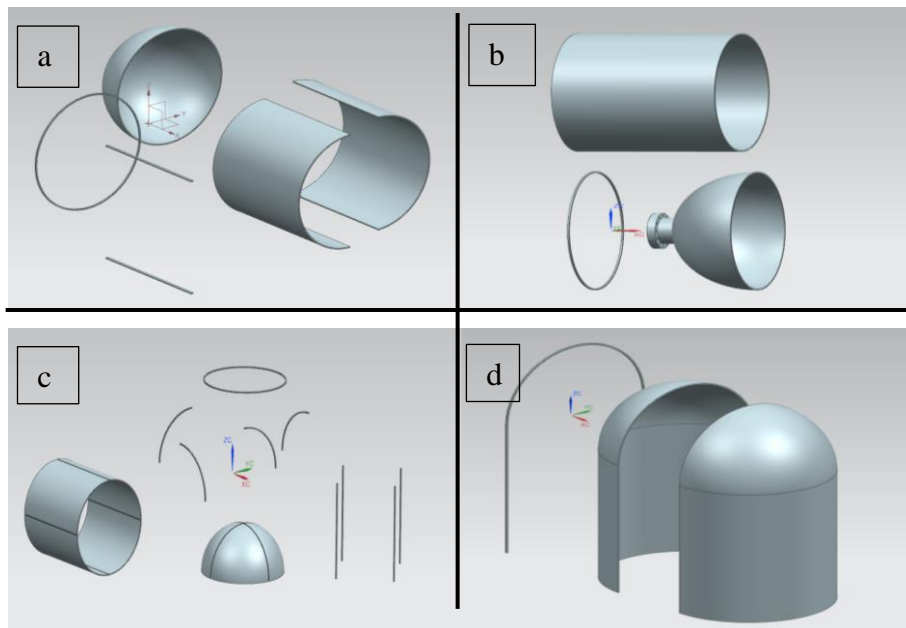


Figure 8. Four weld models created (a) one circular and two straight weld lines, (b) one circular weld line, (c) one circular, four quarter-circle and four straight weld lines, and (d) one U-shape weld line

5.2. Results and Discussion for Weld Geometry and Location

The data presented in

Table 8 reveal that the inclusion of welds in the pressure vessel resulted in an increase in principal stress across all weld models. Among the weld models, weld model b (depicted in **Figure 8**) exhibited the smallest stress increase. Notably, positioning the weld at the joint between the spherical and cylindrical sections of the pressure vessel led to the least stress escalation, with a recorded increase of 5.94 MPa (80.94-75), as shown in

Table 8. It is worth mentioning that the stress measured at the weld location remained below the overall maximum stress recorded in the base model by 19.06 MPa (100-80.94).

Table 8. Results obtained from the weld simulations on the four different weld models compared with the original stress values of the base pressure vessel

Weld Model	Maximum Stress at the Weld (MPa)	Original maximum Stress at the Same Position before the Weld (MPa)
A	150.03	100
B	80.94	75
C	154.69	100
D	136.11	100

It can be observed that the increase in stress exhibited a correlation with the number of welds in each weld model. Weld models B and D, featuring only one weld line, demonstrated the smallest stress increase. Conversely, weld model A, with three weld lines, showed a stress increase of 50 MPa, while weld model C, incorporating nine welds, exhibited a stress increase of 54.69 MPa. This highlights that the presence of more welds in a pressure vessel leads to a greater overall stress increase. Upon scrutinizing the results from each simulation, it became apparent that the inclusion of welds had a more pronounced effect on stress escalation when the weld lines were situated in the cylindrical section, as depicted in **Figure 9** and **Figure 10**.

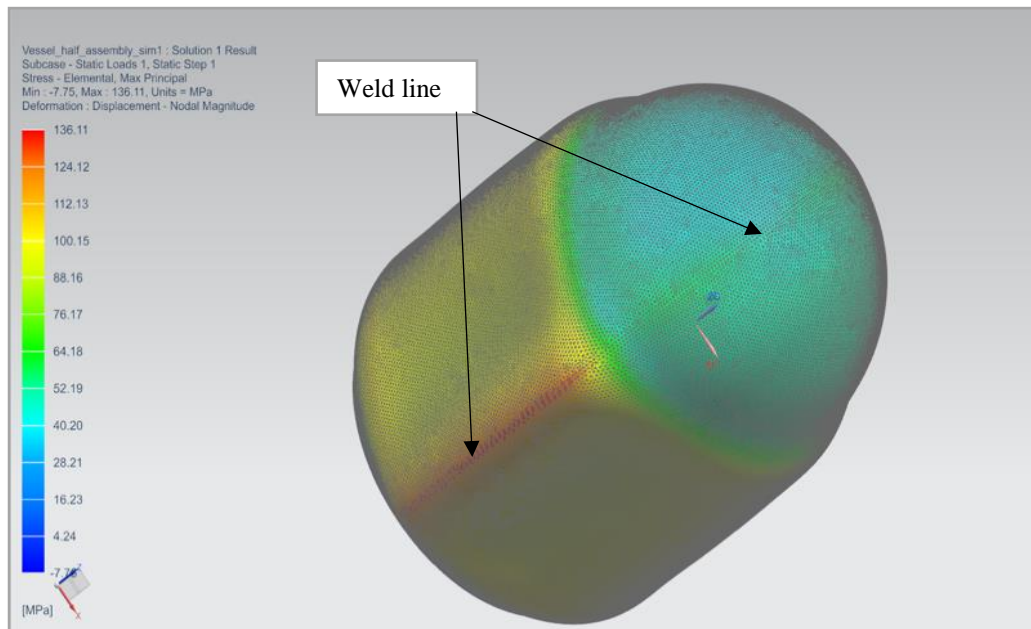


Figure 9. FEA results of weld model D

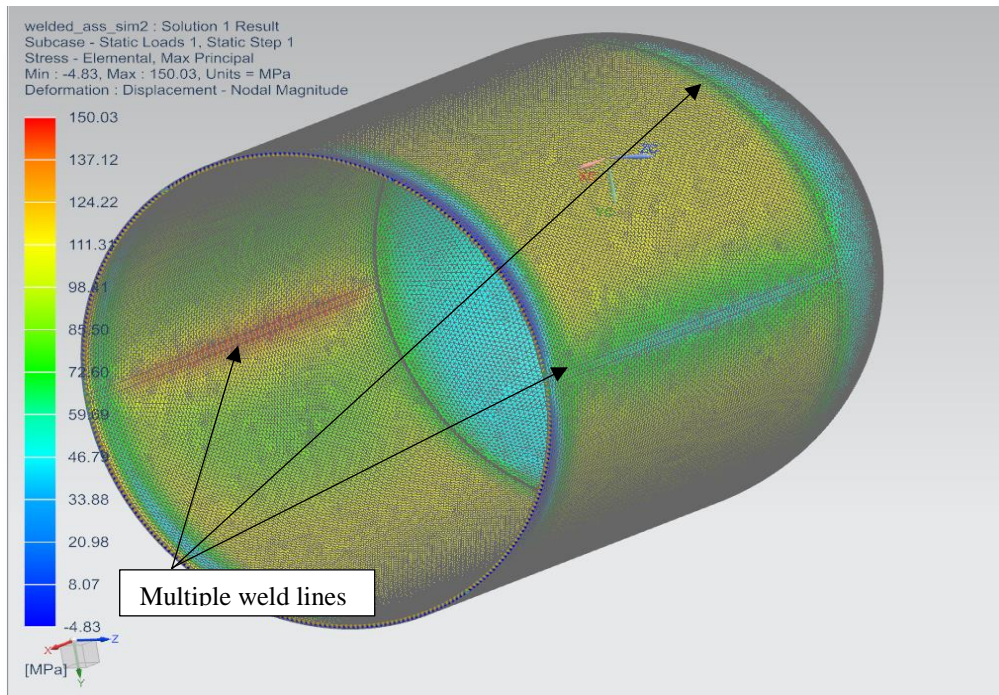


Figure 10. FEA results for weld model A with 3 weld lines

This information holds significance as certain manufacturing companies may encounter limitations in creating weld model B. If they opt for other presented models to manufacture a pressure vessel, they would either need to decrease the maximum working pressure of the vessel or augment the vessel's thickness to adhere to ASME Boiler standards.

6. Optimised Valve Location Including Welds

To further expand on the aforementioned research, it was imperative to investigate whether the inclusion of both welds and valves would lead to any additional stress within the pressure vessel.

6.1. Method

It was decided to utilize the optimal valve location by placing the valve at the centre of the spherical section and incorporate weld locations a, b, and d presented in **Figure 9** to examine the possibility of heightened stress. These three weld models were chosen to provide a broader foundation for identifying any correlations between welds and valves. The three distinct combined models 1, 2, and 3 were crafted in Siemens NX following the methodologies outlined in previous experiments.

Model 1 featured the valve positioned at the centre with the weld located in the same position as weld location model A from prior experiments. Model 2 placed the valve at the centre and

the weld at the same position as weld location model B. Model 3, on the other hand, positioned the valve at the centre with welds situated in the same locations as in weld location model D. Notably, in this model, the weld line intersected the spherical section and the valve to assess any alterations in stress distribution caused by the weld passing through the valve.

6.2. Results and Discussion

From the data presented in

Table 9, it is evident that there were slight discrepancies in the results of models 1 and 3 compared to the welded models A and C from the previous experiment. Model 1 exhibited a stress increase of 0.97 MPa, while model 3 showed a decrease of 1.82 MPa. Interestingly, model 2 displayed no alteration in the maximum recorded stress. Upon closer examination of the Finite Element Analysis (FEA) models, it was observed that the maximum stress values in models 1 and 3 were registered at the weld in the cylindrical section of the vessel. This finding aligns with the results obtained from the weld geometry and location experiments.

Table 9. Results collected from the FEA analysis of welds and a valve in a vessel

Model	Maximum Stress Recorded (MPa)	Maximum Stress Recorded From Previous Weld Geometry Experiment (MPa)	
		presented in	Table 8
1	151.00		150.03
2	100		100
3	134.29		136.11

Figure 11. FEA results of NX model 2 which includes a single weld and a valve at the centre of the spherical section. It can be observed that the stresses at both the weld location (75 MPa) and the valve location (50 MPa) were lower than the longitudinal stress generated in the cylindrical section of the vessel (100 MPa). Once again, this observation mirrors the results obtained from the previous experiment.

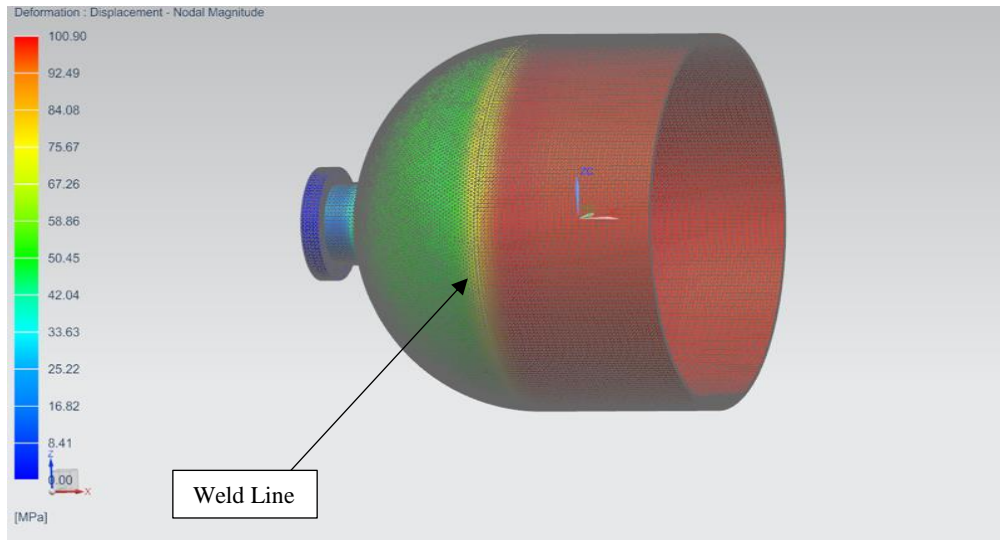


Figure 11. FEA results of NX model 2 which includes a single weld and a valve at the centre of the spherical section

Due to the minimal changes in stress observed in models 1 and 3, and the absence of any change in model 2, it can be inferred that positioning the valve in the centre of the spherical section and incorporating welds did not significantly impact the additional stress induced solely by the welds.

7. Conclusion

The research presented in this paper utilized Finite Element Analysis (FEA) to assess stress distribution in pressure vessel, employing a refined 3D mesh to balance computational efficiency and runtime. The results confirmed that the addition of valves and welds increases localized stresses due to geometric discontinuities. Among the 18 simulated valve positions, placing the valve in the spherical section significantly reduced maximum stress, with the optimal location identified at 0 degree. Analysis of four weld configurations demonstrated that a single weld at the interface between the spherical head and cylindrical body minimizes stress at 80.94 MPa, with a clear correlation observed between the number of welds and increased stress levels. Simulations combining valves and welds revealed no further rise in stress beyond the individual effects of each. These findings provide critical insights into the optimal valve and weld placements for pressure vessel, emphasizing the importance of strategic design in reducing stress concentrations. Additionally, the study highlights discrepancies between calculated and actual stress levels, offering valuable guidance for improving manufacturing processes. Future work could explore experimental validation of the FEA results using strain gauge measurements on physical pressure vessels. Additionally, incorporating fluid-structure

interaction (FSI) simulations could provide deeper insights into the impact of internal fluid dynamics on stress distribution, further enhancing design optimization for real-world applications.

Acknowledgement

The authors would like to thank Teesside University for supporting the research of this study.

Credit Author Statement

Conceptualization and methodology, Grannon, M.; software and validation, Grannon, M., formal analysis, Grannon, M.; investigation, Grannon, M. and Habibi, H.; resources, Grannon, M. and Habibi, H.; data curation, Grannon, M.; writing—original draft preparation, Grannon, M.; writing—review and editing, Habibi, H.; supervision and project administration, Habibi, H.

Conflicts of Interest

The authors declare no conflict of interest.

References

- Bahadur, R., Mittal, V. K., & Angra, S. (2018). Stress analysis of pressure vessel nozzle using FEA. *International Journal of Engineering Research and Technology*, 6(16), 1-6.
- Budynas, R. G., & Nisbett, J. K. (2011). *Shigley's Mechanical Engineering Design* (Vol. 9). New York: McGraw-Hill.
- Diamantoudis, A. T., & Kermanidis, T. (2005). Design by analysis versus design by formula of high strength steel pressure vessels: A comparative study. *International Journal of Pressure Vessels and Piping*, 82(1), 43-50.
- Fricke, S., Keim, E., & Schmidt, J. (2001). Numerical weld modelling - a method for calculating weld-induced residual stresses. *Nuclear Engineering and Design*, 206(2-3), 139-150.
- Hodge, J. C. (1936). The welding of pressure vessels. *Journal of the American Society for Naval Engineers*, 48(4), 498-522.
- Kshitij, K. S., & Sankalp, V. (2019). Structural analysis of weld joints using FEA and response surface optimization. *International Journal for Research in Applied Science and Engineering Technology*, 7(8), 680-688.
- Ladokun, T., Nabhani, F., & Zarei, S. (2010, July). Accidents in pressure vessels: hazard awareness. In *Lecture Notes in Engineering and Computer Science: Proceedings of the World Congress on Engineering 2010*. International Association of Engineers.

- Logan, D. L. (2017). *A first course in the finite element method*. Sixth Edition. Australia: Cengage Learning.
- Megyesy, E. F. (2001). *Pressure vessel handbook*. Twelfth Edition. Tulsa, Oklahoma: Pressure Vessel Publishing.
- Moss, D. R. (1987). *Pressure vessel design manual: illustrated procedures for solving every major pressure vessel design problem*. Houston: Gulf Pub. Co.
- Niranjana, S. J., Patel, S. V., & Dubey, A. K. (2018, June). Design and analysis of vertical pressure vessel using ASME code and FEA technique. In *IOP Conference Series: Materials Science and Engineering* (Vol. 376, No. 1, p. 012135). IOP Publishing.
- Pullarcot, S. K. (2002). *Practical Guide to Pressure Vessel Manufacturing*. CRC Press.
- Romero-Tello, P., Lorente-López, A. J., & Gutiérrez-Romero, J. E. (2025), Structural design optimization of pressure hull using genetic algorithm and finite element analysis. *International Journal of Structural Integrity*, 16(1), 60-84.
- Singh, R. K., Sarda, A., & Chandrakar, P. (2023). A comprehensive study of efficient design of pressure vessels for improved boiler performance. *International Journal of Analytical, Experimental and Finite Element Analysis*, 10(2), 46-49.
- Solangi, E., Albarody, T. M. B., Al-Challabi, S., Khan, J. A., & Ali, S. (2024). Design and failure analysis of a vacuum pressure vessel for aerospace applications using finite element analysis (FEA). *Engineering, Technology & Applied Science Research*, 14(6), 17888–17893.
- Spence, J., & Tooth, A. S. (2012). *Pressure Vessel Design: Concepts and Principles*. CRC Press.